Journal of Orthopaedic Translation 36 (2022) 44–51

Contents lists available at ScienceDirect

Journal of Orthopaedic Translation

journal homepage: www.journals.elsevier.com/journal-of-orthopaedic-translation

Original article

The protective effect of DNA aptamer on osteonecrosis of the femoral head by alleviating TNF-α-mediated necroptosis via RIP1/RIP3/MLKL pathway

Xiaoyu Fan [a], Xin Xu [c], Xinjie Wu [a], Runzhi Xia [c], Fuqiang Gao [b], Qingyu Zhang [d], Wei Sun [a,b,*]

[a] Peking University Health Science Center, China-Japan Friendship School of Clinical Medicine, Beijing, 100029, China
[b] Orthopedics Department, China-Japan Friendship Hospital, Beijing, 100029, China
[c] Peking Union Medical College China-Japan Friendship School of Clinical Medicine, Beijing, 100029, China
[d] Department of Orthopedics, Shandong Provincial Hospital Affiliated to Shandong First Medical University, No.324, Road Jing Wu Wei Qi, Jinan, 250021, Shandong, China

ARTICLE INFO

Keywords:
Aptamer
Bone microvascular endothelial cell
Necroptosis
Osteonecrosis of the femoral head
TNF-α

ABSTRACT

Background: The process of necroptosis mediated by tumor necrosis factor alpha (TNF-α) might play an important role in the onset and development of the osteonecrosis of the femoral head (ONFH). The dysfunctions of bone microvascular endothelial cells (BMECs) have been identified as an important part of pathological processes in the steroid-induced ONFH. An aptamer is a single-stranded DNA or RNA oligonucleotide sequence. Previous studies have designed or screened various aptamers that could bind to specific targets or receptors in order to block their effects.

Objective: There are two main objectives in this study: 1) to establish a TNF-α -induced ONFH model in human BMECs in vitro, 2) to verify the effects of the TNF-α aptamer (AptTNF-α) on blocking TNF-α activity in the ONFH model.

Methods: Clinical samples were collected for Hematoxylin and Eosin (HE) staining, immunohistochemistry and further BMEC isolation. After cell culture and identification, the cell viability of BMECs after incubation with TNF-α was assessed by Cell Counting Kit-8 (CCK8). The necroptosis of BMECs was detected by the TUNEL and Annexin V-FITC/PI staining. The attenuation of TNF-α cytotoxicity by AptTNF-α was evaluated by CCK8 at first. Then, the molecular mechanism was explored by the quantitative real-time polymerase chain reaction and western blotting.

Results: The expression level of TNF-α was significantly up-regulated in bone tissues of ONFH patients. The identification of BMECs was verified by the high expressions of CD31 and vWF. Results from CCK8, TUNEL staining and Annexin V-FITC/PI assay demonstrated reduced cell viability and increased necroptosis of BMECs after TNF-α stimulation. Further investigations showed that TNF-α cytotoxicity could be attenuated by the AptTNF-α in a dose-dependent manner. Necroptosis mediated by TNF-α in the ONFH model was regulated by the receptor-interacting protein kinase 1 (RIPK1)/receptor-interacting protein kinase 3 (RIPK3)/mixed lineage kinase domain-like protein (MLKL) signalling pathway.

Conclusion: We established a TNF-α-induced ONFH model in human BMECs in vitro. Our study also demonstrated that the AptTNF-α could protect BMECs from necroptosis by inhibiting the RIP1/RIP3/MLKL signalling pathway.

The Translational Potential of this Article: The effective protection from cell necroptosis provided by the DNA aptamer demonstrated its translational potential as a new type of TNF-α inhibitor in clinical treatments for patients with ONFH.

1. Introduction

Nontraumatic osteonecrosis of the femoral head (ONFH) is a worldwide challenge for orthopaedic surgeons that may cause long-lasting disability and severe deterioration of patient quality of life. Various risk factors have been identified to be responsible for the onset and development of ONFH, including long-term use of steroids, heavy consumption of alcohol and vascular thrombosis [1,2]. However, the exact

* Corresponding author. Peking University Health Science Center, China-Japan Friendship School of Clinical Medicine, Beijing, 100029, China.
E-mail addresses: Fxy_peking@163.com (X. Fan), 1291271561@qq.com (X. Xu), wuxinjie_ms@163.com (X. Wu), runzhixia@gmail.com (R. Xia), gaofuqiang@bjmu.edu.cn (F. Gao), zqy2008512@163.com (Q. Zhang), sunwei@zryhyy.com.cn (W. Sun).

https://doi.org/10.1016/j.jot.2022.07.001
Received 26 February 2022; Received in revised form 24 June 2022; Accepted 2 July 2022

mechanism of ONFH remains unclear, although many hypotheses have been raised by cell experiments and animal models.

The role of tumour necrosis factor alpha (TNF-α) as a key regulator in balancing cell survival, apoptosis and autophagy has been extensively studied in various cell types and tissues. A previous study suggested that osteoblast apoptosis and autophagy induced by TNF-α might play an important role in ONFH [3]. As a newly recognized cell death type, the role of necroptosis mediated by TNF-α in the development of ONFH has received more attention. Some researchers found that necroptosis is a form of regulated necrotic cell death that is activated under apoptosis-deficient conditions [4]. Yuan et al. found that TNF-α could sensitize neurons in the central neutral system to necroptosis mediated by receptor-interacting protein kinase 1 (RIPK1), receptor-interacting protein kinase 3 (RIPK3) and mixed lineage kinase domain-like protein (MLKL) with relative resistance to apoptosis [5]. Steroid administration is one of the major causes of ONFH. Ichiseki et al. demonstrated that steroid administration in a rabbit model implicated the necroptosis program through the activation of RIP1 and RIP3 [6]. In addition, their results indicated that TNF-α expression was significantly increased in bone tissues affected by ONFH.

Previous reports have identified the important role of BMECs in the development of ONFH caused by microcirculation disorder [7–9]. It has been suggested that BMECs are crucial elements for microcirculation homeostasis, whose dysfunction may initiate apoptosis without physiological angiogenesis [10]. Additionally, previous researchers demonstrated that the disorder of BMECs due to continuous exposure to glucocorticoids was crucial in inducing apoptosis and inhibiting angiogenesis in steroid-induced ONFH [11]. However, there is currently no study on the role of BMECs in necroptosis based on a TNF-α-induced ONFH model.

An aptamer is a single-stranded DNA or RNA oligonucleotide sequence that is capable of binding to specific receptors or targets with high specificity and affinity. Unlike monoclonal antibodies, aptamers bind to a wide range of receptors without triggering the immune system to induce hypersensitivity. Previous studies have implied that various inflammatory cytokines, such as TNF-α and IL-6, might participate in the pathogenesis of ONFH [12]. To date, a total of 11 aptamers have been designed or screened against inflammatory cytokines or related receptors [13]. In a study conducted by Jeong, S. et al., they successfully investigated the Notch1-antagoistic aptamer as a candidate of nucleic acid therapeutics to induce chondrogenic differentiation of human bone marrow stromal cells (BMSCs) [14]. According to recent studies, TNF-α DNA aptamers have been proven to be effective in blocking TNF-α activities in cells and mouse models [15,16]. However, no study was conducted on the blocking capability of TNF-α aptamer in the ONFH model.

2. Materials and methods

2.1. Patients

BMEC specimens were isolated from patients who were hospitalized in the Orthopaedic Department between Feb 2021 and Aug 2021. A total of 30 samples of femoral heads were collected from 15 ONFH patients and 15 control patients (femoral neck fracture within 24 h). All patients received unilateral total hip arthroplasty (THA). We selected the patients diagnosed with femoral neck fracture as the control group for two reasons: 1) it was not proper to choose patients diagnosed with osteoarthritis or rheumatoid arthritis as the control group because of we aimed to study the expression of an inflammatory biomarkers (TNF-α) in clinical samples. 2) we would extract BMECs from the clnical samples of the control group for cell culture. Therefore, patients without any previous bone disorders (except osteoporosis) were expected in the control group. There was no significant difference between the ONFH and fracture groups with regard to sex, age or body mass index. Informed consent documents for femoral head donation were obtained from all enrolled patients, and all the experiments on human samples in our study were approved by the medical ethics committee of the China–Japan Friendship Hospital.

2.2. Haematoxylin and eosin (HE) staining and immunohistochemistry

All collected bone tissues were fixed in 10% formalin for 24 h, after which they were washed with 0.9% saline three times. Then, all samples were decalcified in 10% EDTA decalcifying solution for 3 months.

All paraffin slices were subsequently dehydrated in xylene and various concentrations of ethanol several times before staining with haematoxylin and eosin. After dehydration and sealing, each slice was observed using an electron microscope (LEICA Microsystem, Germany) to examine the necrotic area and its surrounding tissues. The existence of empty lacuna, amorphous substance and trabecular fracture were observed to represent osteonecrosis.

Similar to the first step in HE staining, dehydration was followed by the repair of protease K. The slides were blocked with 3% BSA for 30 min after being washed with PBS three times. The reaction liquid in the TUNEL kit was added to each slide before incubation with primary antibodies and secondary antibodies. The whole processes of HE staining and immunofluorescence staining were previously reported elsewhere [7]. A fluorescence microscope (Olympus, Tokyo, Japan) was used to observe the immunohistochemistry images after sealing with antifade solution.

2.3. BMEC isolation and cell culture

The BMECs in this study were extracted from the enrolled patients diagnosed with femoral neck fracture during surgery under sterile conditions. Briefly, the bone debris was first washed with Dulbecco's modified Eagle's medium (DMEM, Gibco, USA) three times and then digested with 0.2% type I collagenase for 25 min and 0.25% trypsin–EDTA for 5 min at 37 °C. The digestion process was terminated with the addition of DMEM containing 10% foetal bovine serum (FBS). Then, the cell mixture was filtered by a 70 μm cell strainer and centrifuged at 800 rpm for 6 min. Finally, the supernatant was removed, and cells in the deposits were resuspended in 5 ml endothelial cell medium (ECM, ScienCell, USA) for cell counting. BMECs were then cultured in ECM (Gibco BRL, Life Technologies) containing 10% foetal bovine serum (FBS), 1% recombinant human vascular endothelial growth factor (VEGF) and 1% streptomycin-penicillin solution in a 37 °C humidified incubator with 5% CO2. The ECM was replaced every three days, and BMECs were passaged when they reached 80%–90% confluence.

2.4. Identification of BMECs

BMECs were extracted from the cancellous bone of the femoral heads in the control group. Similar to the surface markers of human umbilical vein endothelial cells (HUVECs), CD31 and vWF were selected as the characteristic markers of BMECs [7]. Immunofluorescence staining of the BMECs in 75 ml culture flasks was applied for BMEC identification. As previously reported [17], the blocked cells were incubated with mouse antibodies against CD31 (CST, 1:1000) and vWF (CST, 1:1000) at 4 °C overnight. Then, the anti-rat IgG (H + L) (Alexa Fluor® 488 Conjugate) secondary antibody (CST, 1:2000) was applied for 30 min at 37 °C on the second day. The DAPI and merged images were filmed with a fluorescence microscope (Casse, USA).

2.5. Cell viability via Cell Counting Kit-8 (CCK-8) assay

The ONFH model in BMECs induced by TNF-α was verified by the examination of cell viability and proliferation. The Cell Counting Kit-8 (CCK-8) assay was applied after the incubation of BMECs in 96-well plates along with TNF-α. As previously reported [18], 100 μL of BMECs (2×10^3 cells/well) were seeded into 96-well plates along with TNF-α at concentrations of 500, 100, 50, 25, 12.5 and 6.25 ng/ml. The treated BMECs were cultured at 37 °C for 24 h. Then, 10 μL of CCK-8 solution was

added to each well and incubated at 37 °C for another 2 h in the dark. The OD value of each well was determined by a microplate reader at a wavelength of 450 nm.

2.6. TUNEL staining and Annexin V-FITC/PI for necroptosis detection

Necroptosis was detected using a One Step TUNEL Apoptosis Assay Kit (Beyotime) and an Annexin V-FITC Apoptosis Detection Kit (Beyotime). The cultured cells in the flask were digested and collected in a six-well plate. TNF-α and aptamer at various concentrations were incubated with BMECs at 37 °C for 24 h.

For TUNEL staining, the cells in the plate were washed with phosphate-buffered saline (PBS) three times before fixation in 4% paraformaldehyde for 30 min, immersed in 0.3% Triton X-100 PBS solution for 5 min at room temperature and washed three times with PBS. Finally, the cells were incubated with a TUNEL kit at 37 °C for 1 h in the dark. The whole processes of TUNEL staining were previously reported elsewhere [7]. A fluorescence microscope (Olympus, Tokyo, Japan) was used to observe and capture images at a wavelength of 570 nm for rhodamine.

In the Annexin V-FITC/PI assay, the procedures were taken as previously reported [19]. Cell medium after 24 h of incubation was transferred to a suitable centrifuge tube, and adherent cells were digested by trypsin–EDTA solution. The recycled cell medium was added to the plate to terminate the digestion. Then, the suspension was centrifuged at 1000 rpm for 5 min before discarding the supernatants and resuspending in Annexin V–FITC binding buffer. After incubation with Annexin V-FITC and propidium iodide (PI) in the dark for 20 min, the suspension was analysed by flow cytometry with a FACSCalibur flow cytometer (Becton Dickinson, USA).

2.7. Aptamer preparation and inhibitory effect of TNF-α cytotoxicity

The aptamer applied in this study was obtained from the research conducted by Orava. W [20]. The sequence of the DNA aptamer 'VR11' is 5′-TGG TGG ATG GCG CAG TCG GCG ACA A-3'. The material was synthesized by Sangon Biotech, Shanghai, China. The DNA aptamer was centrifuged at 4000 rpm for 30 s before decapping. Then, 1 ml endothelial cell medium (ECM, ScienCell, USA) was added to dissolve the aptamer at a concentration of 5000 nM. The dissolved aptamer was exposed to a 95 °C metal bath for 3 min and recooled at 4 °C for 10 min before incubation.

BMECs were first cultured in 6-well plates ($2*10^4$ cells each) for 24 h before intervention. Later, TNF-α proteins (200 ng/ml, 100 ng/ml) alone and TNF-α proteins along with aptTNF-α (50, 100, 500 nM) were incubated into each independent well. Aptamers were premixed with human TNF-α proteins at 37 °C for 2 h prior to incubation with BMECs. The inhibitory effect of aptamer on TNF-α cytotoxicity was assessed by the Cell Counting Kit-8 (CCK-8) assay, TUNEL and Annexin V-FITC/PI staining.

2.8. Quantitative real-time polymerase chain reaction (RT–PCR)

After incubation with TNF-α and AptTNF-α for 24 h, total RNA was extracted from BMECs by TRIzol reagent (Invitrogen, USA) and then transcribed into complementary DNA sequences. The primer sequences designed for this study were synthesized by Sangon (Shanghai, China), and the sequence for each gene is shown in Table 1. The expression of target genes was quantified through RT–PCR on an ABI Prism 7900 HT sequence detection system (Applied Biosystems, USA). Thunderbird SYBR qPCR Mix (TOYOBO, Japan) and ReverTra AceqPCR RT Kit (TOYOBO, Japan) were used for the process. The data of the final products were analysed using the $2^{-\Delta\Delta Ct}$ method. The whole processes of quantitative real-time polymerase chain reaction were previously reported elsewhere [21].

2.9. Western blotting analysis

Following the procedures reported before [15], all protein was extracted by RIPA lysis buffer and mixed with 4x loading buffer (Beyotime, China) before degeneration by heating at 100 °C for 5 min. A 5 μg of protein ladder and 20 μg of each sample was added in the vertical PAGE precast gels and then transferred to a PVDF membrane. The membrane was immersed in quick blocking buffer (Beyotime, China) for 20 min and then washed with 10% TBST solution before incubation with primary antibodies against RIP1 (CST, 1:1000), p-RIP1 (CST, Ser166, 1:1000), RIP3 (CST, 1:1000), p-RIP3 (CST, Ser227, 1:1000), MLKL (CST, 1:1000), p-MLKL (CST, Ser358, 1:1000) and GAPDH (CST, 1:1000) overnight at 4 °C. Corresponding secondary antibodies were incubated with membrane for 30 min after being washed with 10% TBST for five times. The immunoblots were visualized with an Electrochemiluminescence system (Tanon, Shanghai, China) and the protein expression level was quantified by ImageJ software.

2.10. Statistical analysis

The data were recorded in the form of mean ± standard deviation. Data analysis between groups was performed on SPSS Statistics 25 (Chicago, IL, USA) using Student's t-test, one-way analysis of variance (ANOVA). All figures were completed on the GraphPad Prism (Version 8.0). A value of $P < 0.05$ was considered to be statistically significant.

3. Results

3.1. The expression of TNF-α was upregulated in bone tissues of ONFH patients

The HE staining samples from patients with ONFH and bone debris extracted from the control group for BMEC isolation are illustrated in Fig. 1A–B. The thickness of the slices was 4 μm for electron microscope. And there were 5 slices for each patient in total, including 1 unstained slice and 1 slice for pre-experiments. The HE staining images showed empty lacuna, amorphous substances and adipocyte infiltration in the ONFH group. In addition, trabecular fracture was observed in the subchondral region of the patients in the ONFH group, while normal trabecular structure and luxuriant osteocytes were observed in the control group (Fig. 1C and D). According to the immunohistochemistry results, the expression of TNF-α (red) in the necrotic regions of the ONFH group was significantly higher than that in the normal regions of the control group (Fig. 1E–G). The mean fluorescence intensity (MFI) of TNF-α was measured to represent its expression level in bone tissue and each group consisted of six slices for data analysis. The localization of the CD31 antibody (green) was used to indicate the distribution of BMECs.

3.2. Culture and identification of BMECs

The identification of BMECs was verified on the first passage (P1) of cells, and all interventions were performed on the second passage (P2) of cells. The typical morphologies of P1 and P2 BMECs are shown in Fig. 2A

Table 1
The sequences of primers designed for this study.

Gene	Forward sequence	Reverse sequence
RIP1	5′-TCCTCGTTGACCGTGAC-3′	5 -GCCTCCCTCTGCTTGTT-3′
RIP3	5′-CCAGCTCGTGCTCCTTGACT-3′	5′-TTGCGGTCCTTGTAGGTTTG-3′
MLKL	5′-TCTCCCAACATCCTGCGTAT-3′	5′-TCCCGAGTGGTGTAACCTGTA-3′
GAPDH	5′-CGCTAACATCAAATGGGGTG-3′	5′-TTGCTGACAATCTTGAGGGAG-3′

RIP1, the receptor-interacting protein kinase 1. RIP3, the receptor-interacting protein kinase 3. MLKL, the mixed lineage kinase domain-like protein. GAPDH, the glyceraldehyde-phosphate dehydrogenase.

and B, respectively. Similar to previous reports, the P1 BMECs exhibited a short spindle, polygon-shaped and cobblestone-like morphology in terms of colony growth [22]. The P2 cells proliferated at a faster rate with similar morphology to the P1 cells. The cultured BMECs isolated from the control group in our study showed a high expression of CD31 and vWF simultaneously (Fig. 2C and D). The verification of BMECs by the two markers justified the purity of our cells (Fig. 2E).

3.3. Reduced cell viability and increased necroptosis of BMECs after TNF-α stimulation

To verify the necrotic effect mediated by TNF-α on human BMECs, the CCK8 assay was performed in a dose-dependent manner. The CCK8 results revealed that TNF-α inhibited BMEC viability in a dose-dependent manner at the optimal concentration of 100 ng/ml for 24 h (Fig. 3A). The addition of 200 ng/ml TNF-α showed no significant difference in cell viability compared with the 100 ng/ml group. Therefore, a dose of TNF-α at 100 ng/mL was selected for subsequent experiments.

In addition to the CCK8 assay, TUNEL staining was also performed to ascertain the effect of TNF-α induction. Compared with the control group, 100 ng/ml TNF-α showed a higher percentage of necroptosis after 24 h of incubation. There was a significant difference between the two groups (Fig. 3B–D). Annexin V-FITC/PI (AVPI) staining was applied to detect necroptosis. The percentage of cell necroptosis showed significant differences among the control, TNF-α and aptamer groups (Fig. 3E). These results indicated that the reduced cell viability and increased necroptosis rate mediated by TNF-α were successfully established in BMECs.

3.4. AptTNF-α attenuated TNF-α cytotoxicity in a dose-dependent manner

We next investigated whether the aptamer could inhibit the effect of TNF-α on BMECs and its optimal concentration in vitro. According to the necrotic effect of TNF-α, 100 ng/mL TNF-α was selected as the control group. The CCK8 assay was first performed to explore the protective effect of AptTNF-α. The results showed that AptTNF-α attenuates TNF-α cytotoxicity in a dose-dependent manner at the optimal concentration of 500 nM (Fig. 4A). The cell viability between the control group and the AptTNF-α at 50 nM group showed no significant difference. Therefore, the AptTNF-α 100 nM and AptTNF-α 500 nM groups were selected for TUNEL staining to compare the necroptosis activities between the two groups. TUNEL staining revealed that both groups showed significantly less necroptosis activity than the control group. The AptTNF-α 500 nM group showed a better inhibitory effect of necroptosis activities on BMECs compared with the AptTNF-α 100 nM group (Fig. 4B–D). Further investigation of Annexin V-FITC/PI (AVPI) staining was performed to evaluate the effect of AptTNF-α. According to the AVPI results, the percentage of cell necroptosis in the AptTNF-α 500 nM group was significantly lower than that in the control and AptTNF-α 100 nM groups (Fig. 4E).

3.5. AptTNF-α suppressed TNF-α-mediated necroptosis via the RIP1/RIP3/MLKL signalling pathway

To further verify the presence of necroptosis in BMECs, the expression levels of RIP1, RIP3 and MLKL were examined by RT–PCR and western blotting. In addition, to explore the potential effects of AptTNF-α on TNF-α-mediated necroptosis, concentration gradients were applied in the intervention. The results from RT–PCR showed that the expression level of RIP1 increased significantly in the TNF-α group compared with the control group. The RIP1 level in the two AptTNF-α groups was found to be significantly lower than that in the TNF-α group. Similarly, the expression levels of RIP3 and MLKL were found to be significantly higher in the TNF-α group than in the control group. The RIP3 and MLKL levels in the AptTNF-α 500 nM group showed a significant decrease compared with those in the AptTNF-α 100 nM group. However, there was no significant difference in the expression level of RIP1 between the AptTNF-α 500 nM and AptTNF-α 100 nM groups, although both groups showed

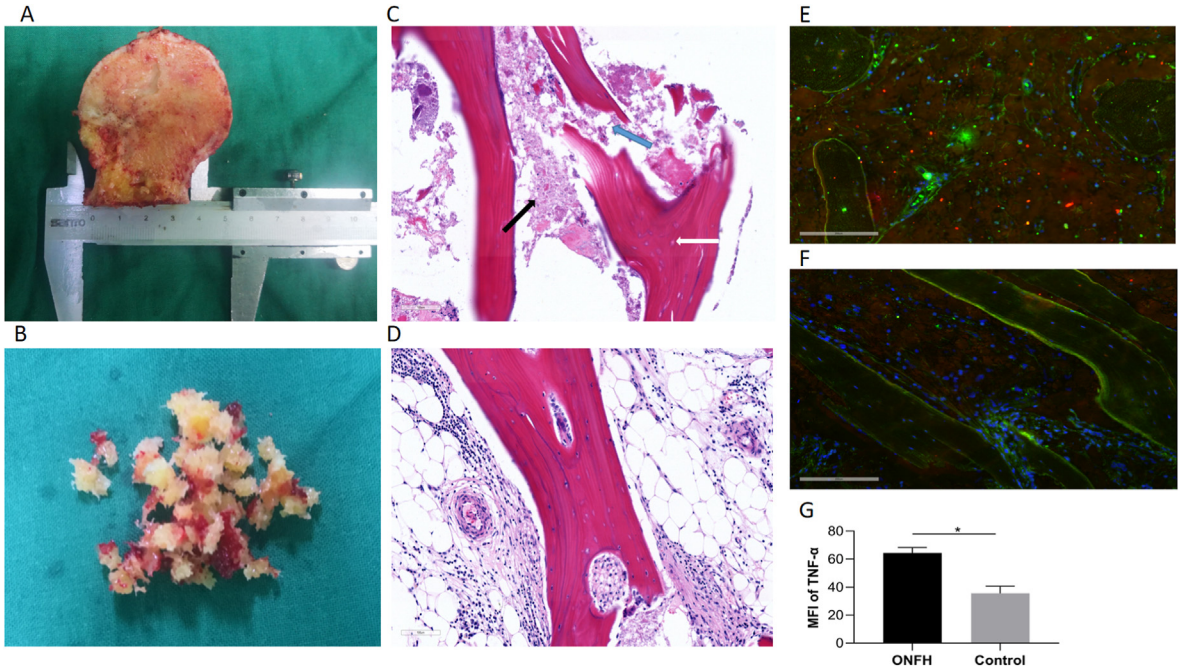

Figure 1. Clinical samples for Hematoxylin and Eosin (HE) staining, immunohistochemistry and BMEC isolation. A, clinical sample of the femoral head in patient with ONFH. B, the bone debris for BMEC isolation which was extracted from the patients with femoral neck fracture. C, the HE staining demonstrated the existence of empty lacuna (white arrow), amorphous substance (black arrow) and trabecular fracture (blue arrow) in the ONFH group. D, the HE staining of the control group. E, Results of the immunohistochemistry in the necrotic regioin. F, Results of the immunohistochemistry in the normal region. G, The mean fluorescence intensity (MFI) of TNF-α (red) in the ONFH and control groups (n = 6, each group consisted of six slices for analysis). *p < 0.05. BMEC, bone microvascular endothelial cell; ONFH, osteonecrosis of the femoral head. (For interpretation of the references to colour in this figure legend, the reader is referred to the Web version of this article.)

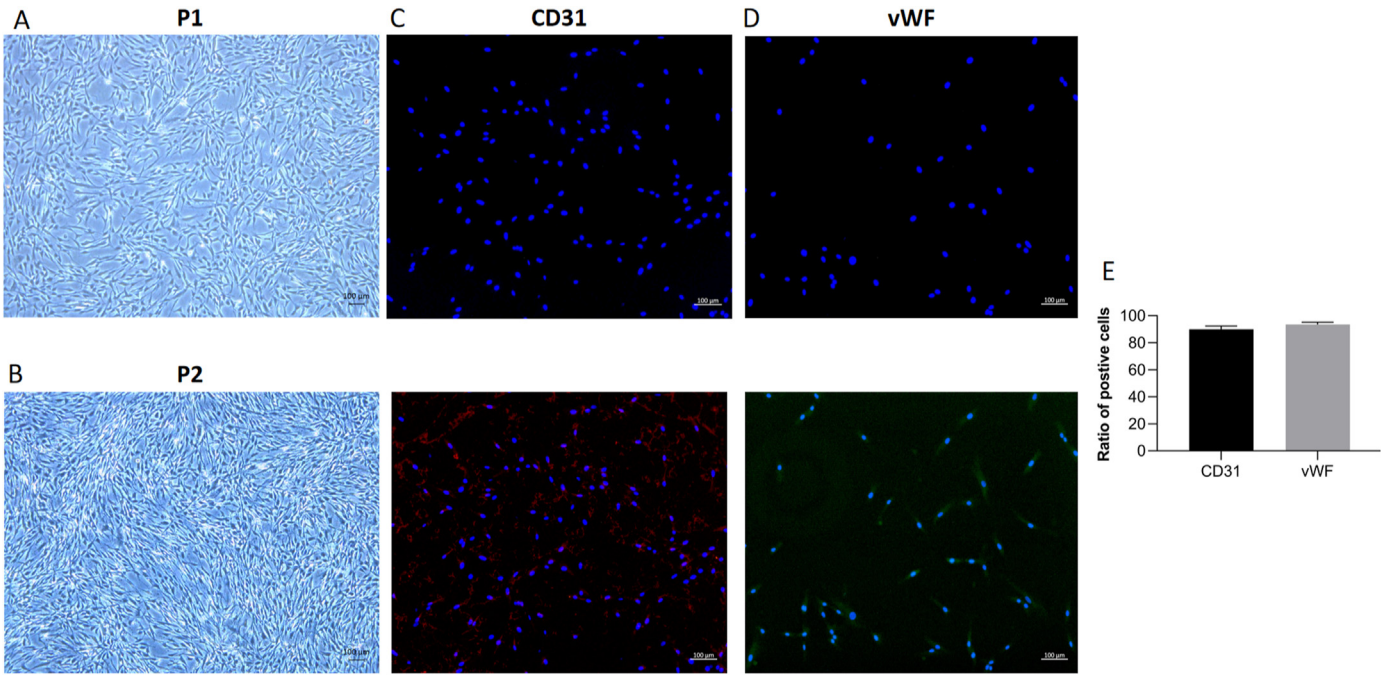

Figure 2. Bone microvascular endothelial cell (BMEC) culture and identification. A,B, The typical morphologies of first passage (P1) and second passage (P2) of BMECs (50 x). C, BMEC identification by the marker of CD31. D, BMEC identification by the marker of vWF. E, the ratio of positive cells in CD31 and vWF staining (n = 3, each group consisted of three repeated wells for analysis).

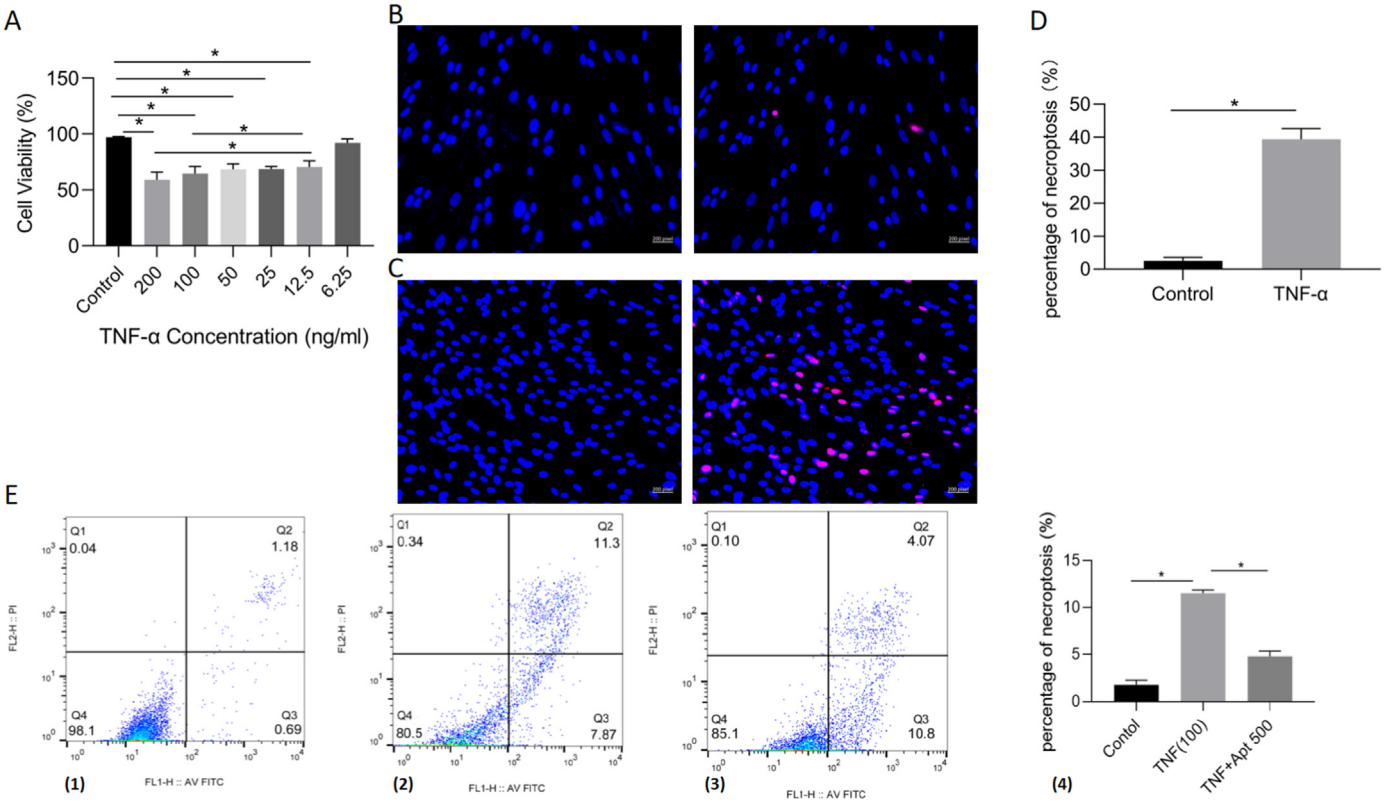

Figure 3. Reduced cell viability and increased necroptosis of BMECs after TNF-α stimulation. A, Cell Counting Kit-8 results of cell viability after incubation with TNF-α for 24 h (n = 3, each group consisted of three repeated wells for analysis). B, the TUNEL staining results of the control group. C, the TUNEL staining results of the 100 ng/ml TNF-α group. D, the percentage of cell necroptosis from the TUNEL staining in the 100 ng/ml TNF-α and control group (n = 3, each group consisted of three repeated wells for analysis). E, (1)–(3) the BMECs were stained with the Annexin V-FITC/propidium iodide (PI) in the control, 100 ng/ml TNF-α and 100 ng/ml TNF-α + 500 nM AptTNF-α group, respectively. The cells in the Q2(UR) and Q1(UL) stand for the percentage of necroptosis. (4) Quantitative data analyses of the Annexin V-FITC/PI results in these three groups (n = 3, each group was repeated three times in six-well plate for analysis). *p < 0.05. BMEC, bone microvascular endothelial cell. Apt 50, 50 nM TNF-α aptamer. Apt 100, 100 nM TNF-α aptamer. Apt 500, 500 nM TNF-α aptamer.

lower values than the blank group (Fig. 5A–C).

The ratio of phosphorylated protein to the original protein was recognized as an important hallmark for the activation of necroptosis. According to the western blotting results, there was no significant difference in the expression level of GAPDH among the four groups. The ratio of phospho-RIP1 (p-RIP1) to RIP1 was found to be significantly increased in the 100 ng/ml TNF-α group but significantly decreased in the AptTNF-α 500 nM and AptTNF-α 100 nM groups. Similar results were observed for the ratio of phospho-RIP1(p-RIP3) to RIP3 and phospho-MLKL (p-MLKL) to MLKL. The ratio of p-RIP1/RIP1, p-RIP3/RIP3 and p-MLKL/MLKL, which was normalized to GAPDH, was significantly decreased in the AptTNF-α 500 nM group compared with the AptTNF-α 100 nM group (Fig. 5D–H).

4. Discussion

In the current study, we established a TNF-α-induced ONFH model in human BMECs in vitro. In addition, we also verified the blocking effect of the TNF-α aptamer (AptTNF-α) on necroptosis in the TNF-α-induced ONFH model. The results from this study suggest the great potential for the application of specific aptamers to be translated into clinical practice for patients with ONFH.

TNF-α-mediated osteoblast differentiation, apoptosis, and necroptosis are triggers for a variety of bone diseases, such as ONFH, osteoporosis, traumatic bone disease, metabolic bone disorders and many inflammatory joint diseases. The key role of TNF-α in the development of ONFH was uncovered in previous studies and confirmed in human cells in vitro in our study. In the first step, we found that TNF-α expression was significantly higher in clinical specimens of ONFH patients than in those of control patients. Therefore, we believe that this finding might provide a novel idea for the development of a new treatment strategy for ONFH, indicating that TNF-α inhibitors may be a good treatment route. There have been a few therapeutics targeting TNF proteins in clinical practice, such as monoclonal antibodies (mAbs). However, there are several limitations in the current therapeutic paradigm of global TNF blockade, the three most important being low rates of disease remission, the development of adverse biological effects and the generation of antibodies against biologic TNF inhibitors [23]. To overcome the drawbacks associated with mAbs, we are seeking alternative agents for the specific detection and targeting of TNF activities without compromising therapeutic effects and reducing cost.

The idea of using single-stranded oligonucleotides as affinity molecules for various target compounds was initially proposed in 1990 [24, 25]. As an antidote for specific receptors, DNA aptamers (single-stranded oligonucleotides) can be easily designed and synthesized. Compared with traditional protein-based inhibitors, such as antibodies, no strict conditions are required for transportation, and fewer immune reactions are triggered. Given the features of small molecules and the low immunogenicity of DNA aptamers, this precise TNF inhibitor could lead to a bright future for clinical treatments if the effective blockade of the TNF signalling pathway is proven. In our study, the TNF-α aptamer (VR11) significantly alleviated the necroptosis of human BMECs induced by TNF-α according to the results of TUNEL staining and AVPI. Compared with the TNF-α intervention alone, as an inhibitor of TNF-α, the aptamer intervention demonstrated higher cell viability and decreased cytotoxicity in vitro. In addition, we found that AptTNF-α attenuated

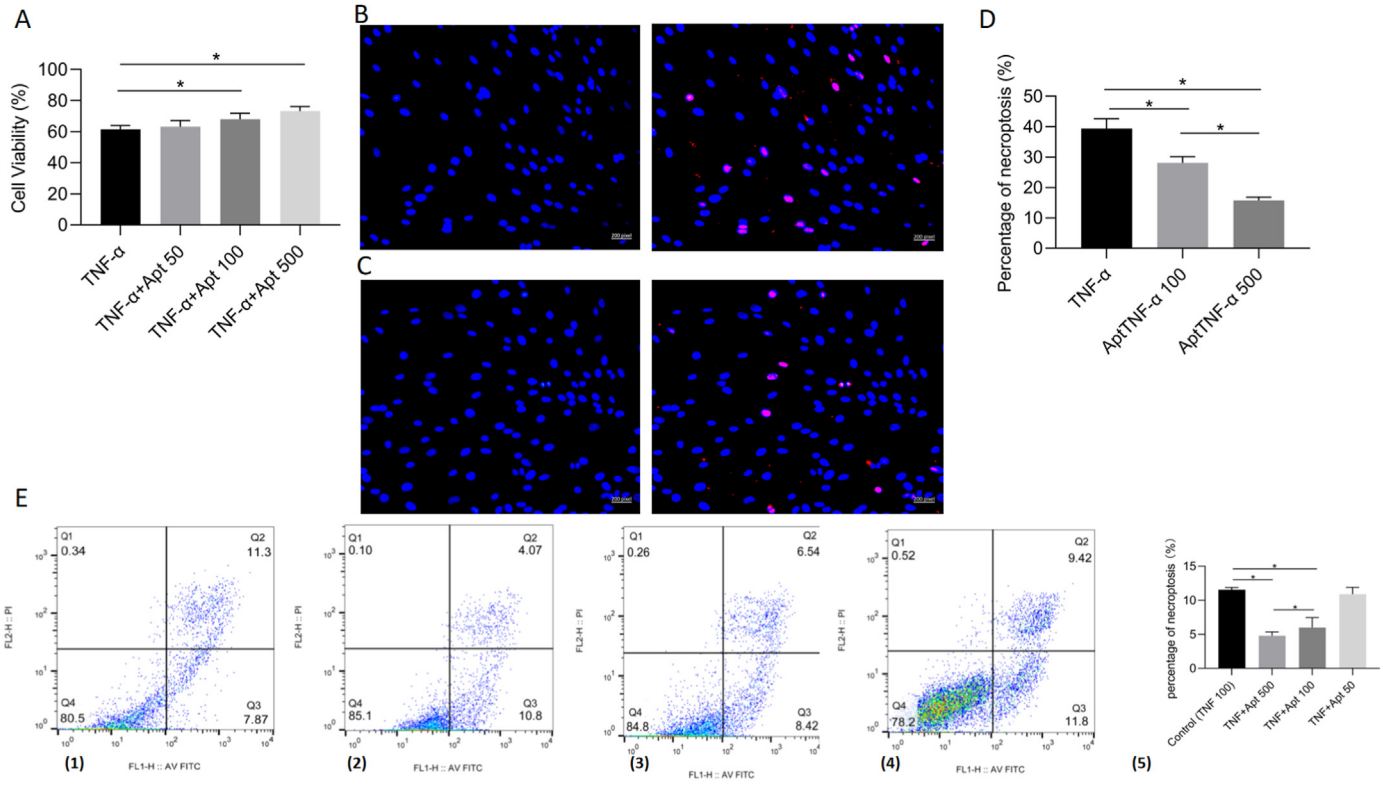

Figure 4. AptTNF-α attenuated TNF-α cytotoxicity in a dose-dependent manner. A, Cell Counting Kit-8 results of cell viability after incubation with TNF-α and AptTNF-α for 24 h (n = 3, each group consisted of three repeated wells for analysis). B, the TUNEL staining results of the 100 ng/ml TNF-α + 100 nM AptTNF-α group. C, the TUNEL staining results of the 100 ng/ml TNF-α + 500 nM AptTNF-α group. D, the percentage of cell necroptosis from the TUNEL staining in 100 ng/ml TNF-α, 100 ng/ml TNF-α + 100 nM AptTNF-α, 100 ng/ml TNF-α + 500 nM AptTNF-α group (n = 3, each group consisted of three repeated wells for analysis). E, (1)–(4) the BMECs were stained with the Annexin V-FITC/propidium iodide (PI) in the 100 ng/ml TNF-α, 100 ng/ml TNF-α + 500 nM AptTNF-α, 100 ng/ml TNF-α + 100 nM AptTNF-α and 100 ng/ml TNF-α + 50 nM AptTNF-α, respectively. The cells in the Q2(UR) and Q1(UL) stand for the percentage of necroptosis. (5) Quantitative data of the Annexin V-FITC/PI results in these four groups (n = 3, each group was repeated three times in six-well plate for analysis). *$p < 0.05$. BMEC, bone microvascular endothelial cell. AptTNF-α, TNF-α aptamer.

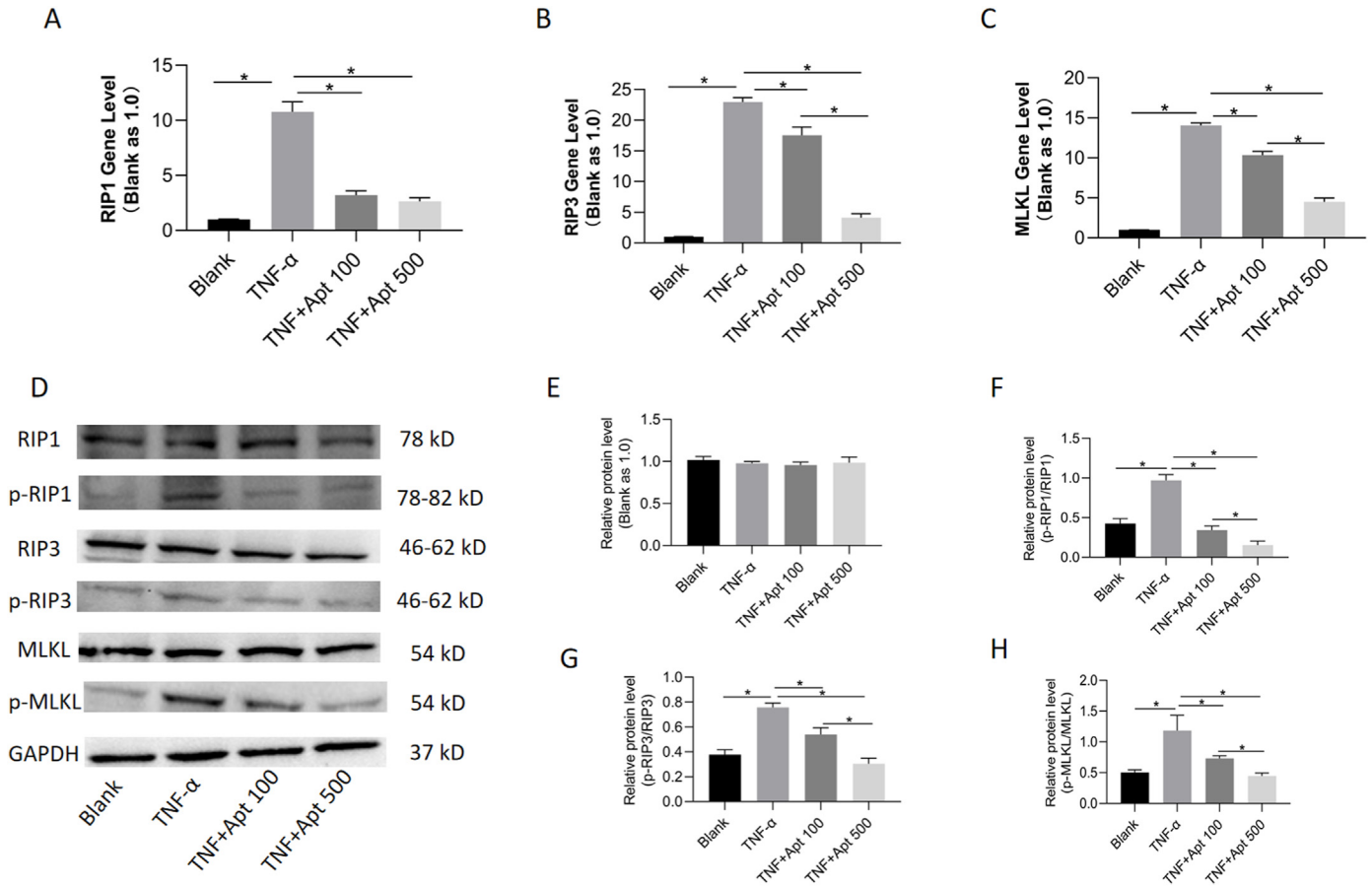

Figure 5. AptTNF-α regulated TNF-α-mediated necroptosis via RIP1/RIP3/MLKL signalling pathway. A,B,C, the mRNA levels of RIPK1, RIPK3 and MLKL gene were measured by RT-PCR after incubation with TNF-α and AptTNF-α for 24 h (n = 3, each group was repeated from three batches of samples for analysis). *p < 0.05. D, Expression level of RIPK1, RIPK3 and MLKL, along with their phosphorylated proteins in the BMECs examined by the Western blotting. E,F,G,H, the relative protein level of GAPDH, p-RIP1/RIP1, p-RIP3/RIP3 and p-MLKL/MLKL from the Western blotting analysis, respectively. The ratio of p-RIP1/RIP1, p-RIP3/RIP3 and p-MLKL/MLKL was normalized to GAPDH (n = 3, each group was repeated from three batches of samples for analysis). *p < 0.05. BMEC, bone microvascular endothelial cell. AptTNF-α, TNF-α aptamer. Apt 100, 100 nM TNF-α aptamer. Apt 500, 500 nM TNF-α aptamer.

TNF-α-induced necroptosis in a dose-dependent manner. This evidence from our study of AptTNF-α demonstrates its protective effect on the development of ONFH while possibly avoiding the adverse events of the current anti-TNF-α agents in clinical therapies.

The necroptosis pathway has been recently recognized, and its regulatory role has been identified in several cell types [4–6,18,21,26]. Necroptosis is a new noncaspase-dependent apoptosis pathway, in a study conducted by Ichiseki et al. their results suggested that necroptosis played an important role in the stage of osteonecrosis development [6]. Furthermore, extensive evidence has revealed the role of TNF as a master regulator in the process of necroptosis, indicating its tremendous importance for mammalian inflammation and cellular homeostasis [27–30]. As shown in our TNF-α-mediated ONFH model in human BMECs, necroptosis was activated through the RIP1-RIP3-MLKL signalling pathway. After incubation with TNF-α, the expression levels of related genes and proteins in this pathway were found to be significantly elevated compared with those in the control group. The western blotting results showed that the phosphorylation of RIP1, RIP3 and MLKL could be an indicator of necroptosis activation. As anticipated, the ratio of phospho-RIP1/RIP3/MLKL to RIP1/RIP3/MLKL was significantly increased in the TNF-α group compared with the control group. The ratio was found to be decreased in the groups coincubated with AptTNF-α and TNF-α protein. With further investigations, we showed that the protective effect of AptTNF-α on cell viability was dose dependent.

5. Conclusion

In summary, we established a TNF-α-induced ONFH model in human BMECs in vitro. The results of our study illustrated that necroptosis was activated via the RIP1/RIP3/MLKL signalling pathway during the development of ONFH. The effective protection from cell necroptosis provided by the DNA aptamer demonstrated its translational potential as a new type of TNF-α inhibitor in clinical treatments for patients with ONFH.

Authors' contributions

Xiaoyu Fan: Conceptualization, methodology, data analyses. **Xin Xu**: Data collection, preparation of the specimens. **Xinjie Wu**: Software, data analyses. **Runzhi Xia**: Data collection and analyses. **Fuqiang Gao**: Software, Validation. **Qingyu Zhang**: Date analyses. **Wei Sun**: Supervised and directed the project. All authors: drafting the article and approval of the final version to be submitted.

Ethics approval and consent to participate

The work described has been carried out in accordance with The Code of Ethics of the World Medical Association (Declaration of Helsinki) for experiments involving human subjects. This study was conducted after

the approval by the Institutional Ethics Review Committee of the China–Japan Friendship Hospital (No. 2021-16-K08, Beijing, China).

Consent for publication

The informed consent was obtained from each patient who provided clinical samples in this study.

Funding

This work was supported by grants from the National Natural Science Foundation of China (grant no. 82072524), the Young Taishan Scholars Program of Shandong Province (QZ,No: tsqn201909183).

Conflicts of interest

A conflict of interest occurs when an individual's objectivity is potentially compromised by a desire for financial gain, prominence, professional advancement or a successful outcome. The Editors of the *Journal of Orthopaedic Translation* strive to ensure that what is published in the Journal is as balanced, objective and evidence-based as possible. Since it can be difficult to distinguish between an actual conflict of interest and a perceived conflict of interest, the Journal requires authors to disclose all and any potential conflicts of interest.

Declaration of competing interest

The authors have no potential financial and non-financial conflicts of interest relevant to this article.

Acknowledgements

All persons who have made substantial contributions to the work reported in the manuscript (e.g., technical help, writing and editing assistance, general support), but who do not meet the criteria for authorship, are named in the Acknowledgements and have given us their written permission to be named. If we have not included an Acknowledgements, then that indicates that we have not received substantial contributions from non-authors.

References

[1] Barquet A, Mayora G, Guimaraes JM, Suárez R, Giannoudis PV. Avascular necrosis of the femoral head following trochanteric fractures in adults: a systematic review. Injury 2014;45:1848–58.
[2] Guerado E, Caso E. The physiopathology of avascular necrosis of the femoral head: an update. Injury 2016;47:S16–26.
[3] Zheng LW, Wang WC, Mao XZ, Luo YH, Tong ZY, Li D. TNF-α regulates the early development of avascular necrosis of the femoral head by mediating osteoblast autophagy and apoptosis via the p38 MAPK/NF-κB signalling pathway. Cell Biol Int 2020;44:1881–9.
[4] Degterev A, Huang Z, Boyce M, Li Y, Jagtap P, Mizushima N, et al. Chemical inhibitor of nonapoptotic cell death with therapeutic potential for ischemic brain injury. Nat Chem Biol 2005;1:112–9.
[5] Yuan J, Amin P, Ofengeim D. Necroptosis and RIPK1-mediated neuroinflammation in CNS diseases. Nat Rev Neurosci 2019;20:19–33.
[6] Ichiseki T, Ueda S, Ueda Y, Tuchiya M, Kaneuji A, Kawahara N. Involvement of necroptosis, a newly recognized cell death type, in steroid-induced osteonecrosis in a rabbit model. Int J Med Sci 2017;14:110–4.
[7] Yu H, Liu P, Zuo W, Sun X, Liu H, Lu F, et al. Decreased angiogenic and increased apoptotic activities of bone microvascular endothelial cells in patients with glucocorticoid-induced osteonecrosis of the femoral head. Bmc Musculoskel Dis 2020:21.
[8] Nishimura T, Matsumoto T, Nishino M, Tomita K. Histopathologic study of veins in steroid treated rabbits. Clin Orthop Relat Res 1997:37–42.
[9] Kerachian MA, Seguin C, Harvey EJ. Glucocorticoids in osteonecrosis of the femoral head: a new understanding of the mechanisms of action. J Steroid Biochem Mol Biol 2009;114:121–8.
[10] Kusumbe AP, Ramasamy SK, Adams RH. Coupling of angiogenesis and osteogenesis by a specific vessel subtype in bone. Nature 2014;507:323–8.
[11] Zhang Y, Yin J, Ding H, Zhang C, Gao YS. Vitamin K2 ameliorates damage of blood vessels by glucocorticoid: a potential mechanism for its protective effects in glucocorticoid-induced osteonecrosis of the femoral head in a rat model. Int J Biol Sci 2016;12:776–85.
[12] Oliveira RA, Fierro IM. New strategies for patenting biological medicines used in rheumatoid arthritis treatment. Expert Opin Ther Pat 2018;28:635–46.
[13] Boshtam M, Asgary S, Kouhpayeh S, Shariati L, Khanahmad H. Aptamers against pro- and anti-inflammatory cytokines: a review. Inflammation 2017;40:340–9.
[14] Jeong S, Kang M, Kim J, Im G. Notch1-antagonistic aptamer for chondrogenic differentiation of bone marrow stromal cells. J Orthop Transl 2016;7:134–5.
[15] Lai W, Wang J, Huang B, Lin EP, Yang P. A novel TNF-α-targeting aptamer for TNF-α-mediated acute lung injury and acute liver failure. Theranostics 2019;9:1741–51.
[16] Mashayekhi K, Ganji A, Sankian M. Designing a new dimerized anti human TNF-α aptamer with blocking activity. Biotechnol Prog 2020;36.
[17] Wu X, Wang Y, Fan X, Xu X, Sun W. Extracorporeal shockwave relieves endothelial injury and dysfunction in steroid-induced osteonecrosis of the femoral head via miR-135b targeting FOXO1: in vitro and in vivo studies. Aging (Albany NY) 2022;14:410–29.
[18] Wang Y, Zhao M, He S, Luo Y, Zhao Y, Cheng J, et al. Necroptosis regulates tumor repopulation after radiotherapy via RIP1/RIP3/MLKL/JNK/IL8 pathway. J Exp Clin Cancer Res 2019;38.
[19] Ji X, Xu F, Dong G, Jia C, Jia P, Chen H, et al. Loading necrostatin-1 composite bone cement inhibits necroptosis of bone tissue in rabbit. Regenerative Biomaterials 2019;6:113–9.
[20] Orava EW, Jarvik N, Shek YL, Sidhu SS, Gariépy J. A short DNA aptamer that recognizes TNFα and blocks its activityin vitro. ACS Chem Biol 2013;8:170–8.
[21] Chen S, Lv X, Hu B, Shao Z, Wang B, Ma K, et al. RIPK1/RIPK3/MLKL-mediated necroptosis contributes to compression-induced rat nucleus pulposus cells death. Apoptosis 2017;22:626–38.
[22] Gao F, Mao T, Zhang Q, Han J, Sun W, Li Z. H subtype vascular endothelial cells in human femoral head: an experimental verification. Ann Palliat Med 2020;9:1497–505.
[23] Kalliolias GD, Ivashkiv LB. TNF biology, pathogenic mechanisms and emerging therapeutic strategies. Nat Rev Rheumatol 2016;12:49–62.
[24] Tuerk C, Gold L. Systematic evolution of ligands by exponential enrichment: RNA ligands to bacteriophage T4 DNA polymerase. Science 1990;249:505–10.
[25] Ellington AD, Szostak JW. In vitro selection of RNA molecules that bind specific ligands. Nature 1990;346:818–22.
[26] Xu Y, Gao H, Hu Y, Fang Y, Qi C, Huang J, et al. High glucose-induced apoptosis and necroptosis in podocytes is regulated by UCHL1 via RIPK1/RIPK3 pathway. Exp Cell Res 2019;382:111463.
[27] Blaser H, Dostert C, Mak TW, Brenner D. TNF and ROS crosstalk in inflammation. Trends Cell Biol 2016;26:249–61.
[28] Kim YS, Morgan MJ, Choksi S, Liu ZG. TNF-induced activation of the Nox1 NADPH oxidase and its role in the induction of necrotic cell death. Mol Cell 2007;26:675–87.
[29] Bae YS, Oh H, Rhee SG, Yoo YD. Regulation of reactive oxygen species generation in cell signalling. Mol Cell 2011;32:491–509.
[30] Dai Q, Zhang Y, Liao X, Jiang Y, Lv X, Yuan X, et al. Fluorofenidone alleviates renal fibrosis by inhibiting necroptosis through RIPK3/MLKL pathway. Front Pharmacol 2020;11.